Inorganic Chemistry

Article

pubs.acs.org/IC

Anticancer C,N-Cycloplatinated(II) Complexes Containing Fluorinated Phosphine Ligands: Synthesis, Structural Characterization, and Biological Activity

Natalia Cutillas,[†] Alexandra Martínez,[†] Gorakh S. Yellol,[†] Venancio Rodríguez,[†] Ana Zamora,[†] Mónica Pedreño,[†] Antonio Donaire,[†] Christoph Janiak,[‡] and José Ruiz*[,†]

[†]Departamento de Química Inorgánica and Regional Campus of International Excellence "Campus Mare Nostrum", Universidad de Murcia and Instituto Murciano de Investigación Biosanitaria (IMIB), E-30071 Murcia, Spain

[‡]Institut für Anorganische Chemie und Strukturchemie, Universität Düsseldorf, Universitätsstrasse 1, D-40225 Düsseldorf, Germany

Supporting Information

ABSTRACT: A series of potent C,N-cycloplatinated(II) phosphine antitumor complexes containing fluorous substituents in the cyclometalated or the ancillary phosphine ligands [Pt(C−N)(PR_3)Cl] or both have been synthesized and characterized. The crystal structure of [Pt(dmba){P-($C_6H_4CF_3$-p)$_3$}Cl]·2CH_2Cl_2 (dmba = dimethylaminomethyl)-phenyl) has been established by X-ray diffraction. Values of IC_{50} of the new platinum complexes were calculated toward a panel of human tumor cell lines representative of ovarian (A2780 and A2780cisR) and breast cancers (T47D). Complexes containing P($C_6H_4CF_3$-p)$_3$ as ancillary ligand (with a bulky and electronegative CF_3 substituent in *para* position) were the most cytotoxic compounds in all the tested cancer cell lines. In some cases, the IC_{50} values were 16-fold smaller than that of cisplatin and 11-fold smaller than the non-fluorous analogue [Pt(dmba)(PPh_3)Cl]. On the other hand, very low resistance factors (RF) in A2780cisR (cisplatin-resistant ovarian carcinoma) at 48 h were observed (RF ≈ 1) for most of the new compounds. Analysis of cell cycle was done for the three more active compounds in A2780. They arrest cell growth in G0/G1 phase in contrast to cisplatin (S phase) with a high incidence of late-stage apoptosis. They are also good cathepsin B inhibitors (an enzyme implicated in a number of cancer related events).

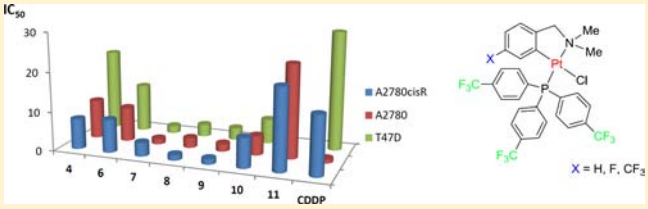

INTRODUCTION

The discovery of the antitumoral drug cisplatin by B. Rosenberg in the 1960s revolutionized cancer chemotherapy. Although many cisplatin analogues have been biologically evaluated, few possess pharmacological advantages relative to cisplatin. In fact, only three platinum-based anticancer drugs (cisplatin, carboplatin, and oxaliplatin) have been approved worldwide, and they are still used in more than 50% of the treatment regimens for cancer patients. The global market of platinum-based drugs represents several billion euro. Yet, platinum drugs are untargeted, their use is often accompanied by severe side effects such as nephrotoxicity, and they are often prone to resistance mechanisms.[1−3] Consequently, circumvention of the aforementioned limitations of cisplatin is a challenge in pharmaceutical research.[4−14]

On the other hand, the unique properties of fluorine render the presence of fluoro substituents an excellent choice to modify the electronic properties and hydrophobicity of the resulting platinum complexes especially through the use of trifluoromethyl groups.[15,16] In fact, fluorine has emerged as a "magic element" in medicinal chemistry as well as in crop and materials science.[17]

We report herein the synthesis and cytotoxic activity of a series of new nonconventional C,N-cycloplatinated(II) phosphine antitumor complexes containing fluorous substituents in the cyclometalated or the ancillary phosphine ligands or both of the type [Pt(C−N)(PR_3)Cl]. Values of IC_{50} were studied for the new platinum(II) complexes against a panel of human tumor cell lines representative of ovarian (A2780 and A2780cisR), and breast cancer (T47D, cisplatin resistant). Analysis of cell cycle, apoptosis, and accumulation studies were done for the more active compounds in A2780. The interaction of the new Pt(II) complexes toward DNA, and also their behavior as cathepsin B inhibitors (a type of enzyme that is overexpressed in many cancer cell lines) have also been studied.

RESULTS AND DISCUSSION

Synthesis of the New Platinum(II) Compounds [Pt(N−C)(PR_3)Cl], 5−11. The cycloplatinated(II) complexes (Chart 1) were prepared from the reaction of the dinuclear precursor [Pt(N−C)Cl]$_2$ (**1**−**3**; N−C = *C*,*N*-dimethylbenzylamine like ligand) with the corresponding phosphine in 1:2.1 molar ratio in CH_2Cl_2. All the complexes were characterized by ^{1}H, ^{13}C, ^{31}P, ^{19}F, and ^{195}Pt NMR spectroscopy and positive-ion ESI-MS and gave satisfactory elemental analyses. ^{1}H resonances

Received: August 1, 2013
Published: November 14, 2013

Chart 1

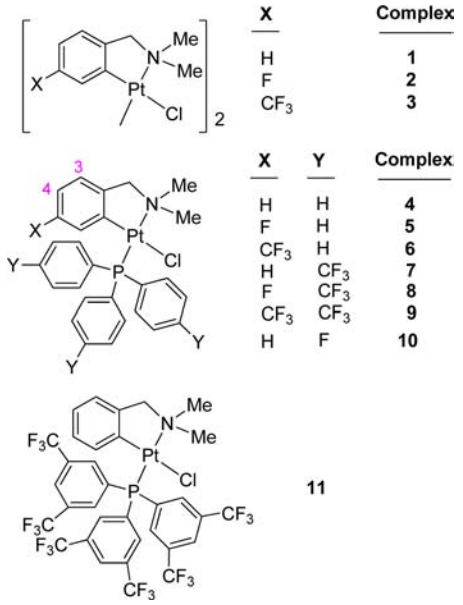

assigned to the methyl groups and the CH_2 group and H^3 of the dmba ligand for **5**–**11** are flanked by ^{195}Pt satellites (see Experimental Section). The assignments were confirmed also by 2D ^1H–^1H NOESY (Supporting Information, Figure S1, for **11**), 2D ^1H–^1H COSY, and HSQC. A NOE effect between H^o protons of PAr_3 with H^3 of dmba is observed, which indicates an R_3P-*trans*-to-NMe_2 ligand geometry for the new monomeric compouds.

X-ray Crystal Structure of Complex 7·2CH_2Cl_2. The crystal structure of 7·2CH_2Cl_2 has been established by X-ray diffraction (Figure 1) with CH_2Cl_2 molecules filling the voids in

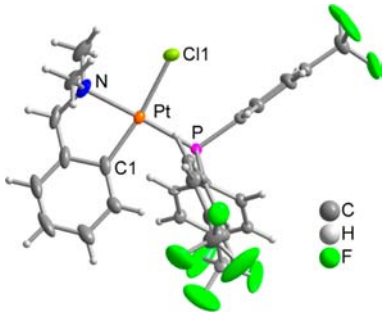

Figure 1. ORTEP plot (ellipsoids drawn at 50% probability level) of complex 7·2CH_2Cl_2. Selected bond lengths (Å) and angles (deg): Pt–C1 = 2.019(9), Pt–N = 2.131(7), Pt–P = 2.212(2), Pt–Cl1 = 2.378(2), C1–Pt–N = 81.6(4), C1–Pt–P = 96.2(3), N–Pt–P = 177.8(2), C1–Pt–Cl1 = 169.8(2), N–Pt–Cl1 = 90.3(2), P–Pt–Cl1 = 91.95(7).

the crystal lattice (Figure S2 in Supporting Information). The Pt atom is in a distorted square planar environment, C–Pt–N bite angle deviating from 90° due to the bite of the cyclometalated ligand.[17,18] As it was suggested from NMR solution studies, the $P(C_6H_4CF_3\text{-}p)_3$ ligand is positioned *trans* to the NMe_2 group, which automatically positions the chlorido ligand *trans* to the aryl ring of the C,N-chelate. The values of the Pt–C and Pt–N bond distances of the bonded dmba ligand are within the normal ranges expected for such cyclometalated complexes.[19] The Pt–P bond length is a bit shorter than that observed in several PPh_3 analogues.[20,21] In the crystal, a rather complex three-dimensional supramolecular network structure is observed built up by extensive hydrogen bonding, which involves weak intermolecular F···H–C[22,23] (Figure S3, Supporting Information) and Cl···H–C contacts[24] and C–H/π interactions (Figure S4, Supporting Information).[25] There are also intermolecular F···Cl contacts (Figure S4, Supporting Information).[26]

Biological Activity: Cytotoxicity Studies. The cytotoxicity of the new platinum(II) complexes **5**–**11** was evaluated (Table 1 and Figure 2) toward the T47D human breast cancer

Table 1. IC_{50} (μM) and Resistance Factors for Cisplatin and Compounds 4–11

complex	T47D 48 h	A2780 48 h	A2780cisR 48 h (RF)[a]
4	20.55 ± 1	9.72 ± 1	7.78 ± 0.6 (0.8)
5	>100	>100	>100
6	12 ± 0.04	8.69 ± 0.06	8.44 ± 0.03 (1.0)
7	1.84 ± 0.07	1.41 ± 0.16	3.48 ± 0.06 (2.5)
8	3.07 ± 0.04	2.50 ± 0.16	1.37 ± 0.08 (0.5)
9	3.03 ± 0.04	1.94 ± 0.17	1.36 ± 0.06 (0.7)
10	6.22 ± 0.04	4.96 ± 0.02	7.61 ± 0.19 (1.5)
11	>100	23.64	20.63 (0.9)
cisplatin	30 ± 2	1.04 ± 0.07	15 ± 1 (14.4)

[a]The numbers in parentheses are the resistance factors, RF (IC_{50} resistant/IC_{50} sensitive).

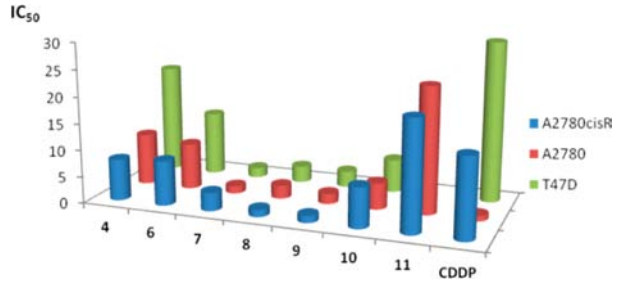

Figure 2. Toxicity of cisplatin and some of the monomeric complexes (IC_{50}, μM) in ovarian and breast cell lines.

cell line (cisplatin resistant) and epithelial ovarian carcinoma cells A2780 and A2780cisR (acquired resistance to cisplatin). The cytotoxicity of the nonfluorinated analogue **4** was also studied for comparison purposes. Because of low aqueous solubility of **4**–**11**, the test compounds were dissolved in DMSO first and then serially diluted in complete culture medium such that the effective DMSO content did not exceed 1%. Complexes **7**–**9**, which contain the $\{P(C_6H_4CF_3\text{-}p)_3\}$ ligand, were the most cytotoxic compounds in all the tested cancer cell lines, the IC_{50} value for complex **7** in T47D being 16-fold smaller than that of cisplatin and 11-fold smaller than the nonfluorous analogue [Pt(dmba)(PPh_3)Cl]. The IC_{50} value for **7** in A2780 is of the same order of magnitude as cisplatin. On the other hand, A2780cisR encompasses all of the known major mechanisms of resistance to cisplatin: reduced drug transport,[27] enhanced DNA repair/tolerance,[28] and elevated GSH levels.[29] The ability of complexes **6**–**11** to circumvent cisplatin acquired resistance was determined from the resistance factor (RF) defined as the ratio of IC_{50} of the resistant line to IC_{50} of the parent line, very low RF values being observed at 48 h (RF = 0.5–1.0, Table 1 and Figure 3), a RF of <2 was considered to denote non-cross-resistance.[30]

dx.doi.org/10.1021/ic401973k | *Inorg. Chem.* 2013, 52, 13529–13535

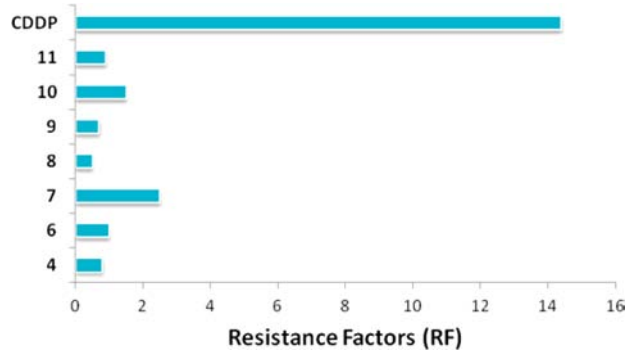

Figure 3. Resistance factors, RF, for cisplatin and some of the monomeric complexes toward cisplatin-resistant A2780 human ovarian cancer cells (A2780cisR).

The stability of the cytotoxic compounds **6**–**11** was tested in DMSO-d_6/DMSO (1:2) by ^{1}H NMR, no free phosphine ligand being detected after 7 days at room temperature. Also no free ligand was present in a mixture containing any of compounds **6**–**11** in the presence of an excess of NaCl (100 mM) after 24 h in solution at 37 °C.

Cell Cycle Arrest. The effect of some of these compounds on cell cycle was examined by dyeing DNA with propidium iodide (PI) and measuring the fluorescence. A2780 cells were treated with compounds **7**, **8**, and **9** at IC_{50} concentrations for 48 h. Then, incubation with PI in the presence of RNase followed. Figure 4 shows the obtained results. A slight increase in G0/G1 phase was observed for the three compounds with respect to control cells (1.8%, 4.2%, and 6.4%, respectively). S and G2 decrement were substantially equal. The arrest of cell cycle in G0/G1 phase contrasts with CDDP behavior previously described.[31]

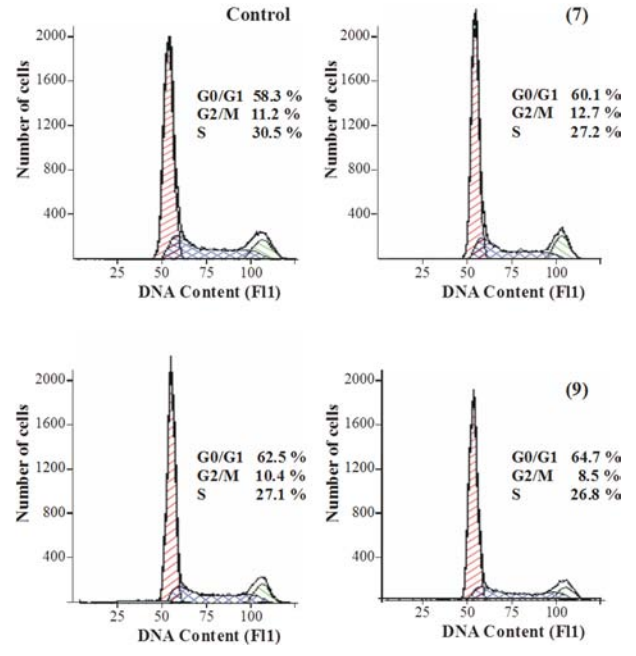

Figure 4. Cell cycle arrest results for A2780 cells without (control) and with previous treatment with compounds **7**–**9**. Integrated areas and fit with the ModFitLT package are printed under the experimental curve. Percentages for each phase of the cell cycle are given in each figure.

Apoptosis Assay. A2780 cell lines were exposed to compound **9** for 48 h. Afterward, a flow cytometric assay was carried out by applying annexin V (Roche) and PI. Fluorescence of both dyes for each cell was measured by flux cytometry. Control and **9** treated cells are shown in Figure 5. An acute increment (from 3.8% to 77.5%) in the D4 (late apoptosis) quadrant is clearly observed. Thus, this compound strongly induces apoptosis in ovarian cancer cells.

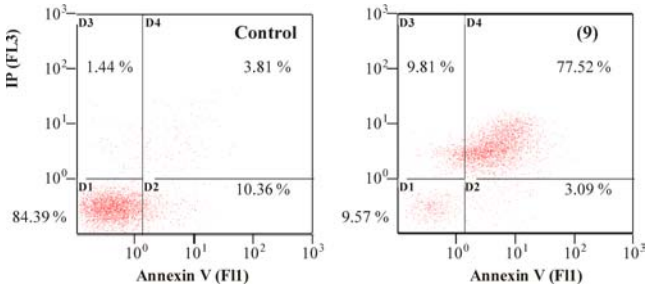

Figure 5. Annexin V and propidium iodide fluorescence intensities for A2780 control (left) and compound **9** treated (right) cells. Viable (D1 quadrant), early apoptotic (D2), necrotic (D3), and late apoptotic (D4) percentages are indicated.

Platinum Accumulation. We have also measured platinum accumulation inside A2780 cells when they were exposed to complex **9** for up to 4 h. Figure 6 shows the obtained results. As a comparison, cisplatin accumulation was 0.71 ± 0.13 ng/10^6 cells in the same conditions. Thus, compound **9** has a much stronger capability to penetrate into these cells.

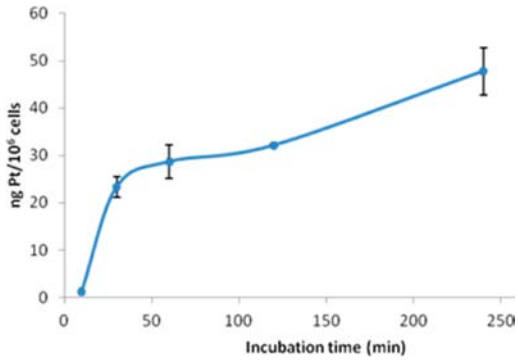

Figure 6. Intracellular platinum accumulation in A2780 cells for up to 240 min incubation with complex **9**.

Biological Assays: Gel Electrophoresis of Compound–pBR322 Complexes. The influence of the compounds on the tertiary structure of DNA was determined by their ability to modify the electrophoretic mobility of the covalently closed circular (ccc) and open (oc) forms of pBR322 plasmid DNA. The compounds **6**–**11** were incubated at the molar ratio r_i = 0.50 with pBR322 plasmid DNA at 37 °C for 24 h. Representative gel obtained for the new compounds **6**–**11** is shown in Figure 7. The behavior of the gel electrophoretic mobility of both forms, ccc and oc, of pBR322 plasmid and DNA/cisplatin adducts is consistent with previous reports.[32]

Reactions of the Platinum(II) Complexes with 9-Ethylguanine. The reactions were carried out in D_2O and DMSO-d_6 (5%) as solvents and followed by ^{1}H NMR (for **7** and **10**) or ESI-MS spectrometry (for **6**–**10**). For NMR studies, the model nucleobase 9-EtG was incubated with the

dx.doi.org/10.1021/ic401973k | Inorg. Chem. 2013, 52, 13529–13535

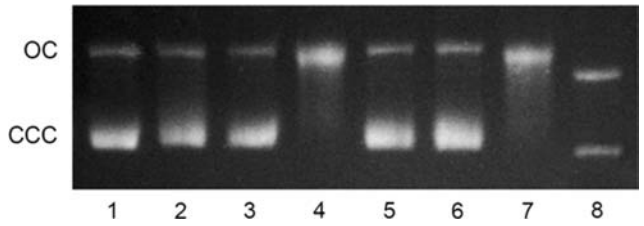

Figure 7. Electrophoretic mobility pattern of pBR322 incubated with the compounds: lane 1, pBR322; lane 2, complex **7**; lane 3, complex **11**,; lane 4, complex **10**; lane 5, complex **9**; lane 6, complex **8**; lane 7, complex **6**; lane 8, CDDP.

new monomeric platinum complexes in a ratio 2:1 at 37 °C for 24 h, the substitution reaction being completed in 30 min (except for complexes **5** and **11**). No further changes were observed after 24 h. In all cases, the ^{1}H NMR signal for the H(8) of the free guanine moves downfield upon coordination (Figure S5, Supporting Information, for the reaction of complex **7**). The ratio coordinated H8 of EtG/$H_{aromatic}$ of C,N agrees well with the formation of the monoadduct with 9-EtG. This was further confirmed by ESI-MS (ratio of 9-ethylguanine was 5:1, Figure S6, Supporting Information, for the reaction of complex **7**).

***In Vitro* Biological Evaluation for Activity against Bovine Cathepsin B.** Cathepsin B (cat B) is an abundant and ubiquitously expressed cysteine peptidase of the papain family. Increased expression and secretion of cat B have been shown to be causally involved in immigration and invasion of numerous human and experimental tumors,[33] and cat B is a possible therapeutic target for the control of tumor progression, and in this respect, it is not surprising that the use of cat B inhibitors reduces both tumor cell mobility and invasiveness in vitro.[34] Recently, some metal complexes were shown to be effective inhibitors of cat B.[35] Complexes **7**−**9** were evaluated for activity against bovine cat B, and the *in vitro* IC_{50} data are reported in Table 2. These values indicate that **7**−**9** are good cathepsin B inhibitors, showing values of the same order of magnitude than RAPTA-C.[35] Figure 8 shows the reduction of enzyme activity as a function of inhibitor concentration for compound **7**. In addition, the cysteine reactivation properties were evaluated for **7** to characterize the reversibility of inhibition (Figure S7, Supporting Information). It was found that the addition of 1 mM cysteine results in full recovery of activity within 2 h. However, after 4 h of incubation some of the activity of the enzyme is lost.

Table 2. In Vitro Biological Data for 7−9 against Bovine Cat B

compound	IC_{50} (μM) vs Cat B
7	8.05 ± 1.2
8	7.68 ± 1.9
9	8.09 ± 1.3

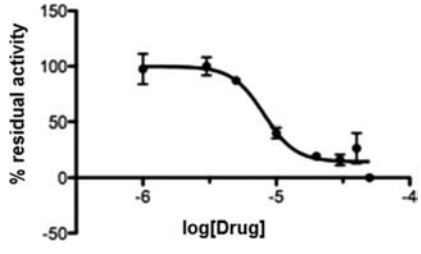

Figure 8. Cat B activity inhibition curve for complex **7**.

CONCLUSIONS

We have successfully synthesized new antitumor *C,N*-platinum(II) complexes [Pt(C−N)(PR_3)Cl] based on *N,N*-dimethylbenzylamine containing fluoro substituents in the cyclometalated or the ancillary phosphine ligands or both. Complexes **7**−**9** containing P($C_6H_4CF_3$-p)$_3$ (with a bulky and electronegative CF_3 substituent in *para* position) are the most cytotoxic compounds in all the tested cancer cell lines. Very low RF values in A2780cisR were observed for **6**−**11**, indicating efficient circumvention of cisplatin resistance. Accumulation studies show that compound **9** has a much stronger ability to penetrate into these cells than cisplatin, probably due to the hydrophobic nature of the fluoro substituents. Reactivity of **6**−**10** toward 9-EtG denotes that DNA is the probable target for these complexes. In A2780 cells, complexes **7**−**9** arrest cell growth in G0/G1 phase, in contrast to cisplatin (S phase), with a high incidence of late-stage apoptosis suggesting a different mechanism of action from that of cisplatin. Additionally, complexes **7**−**9** are good cathepsin B inhibitors, supporting their probable involvement in inhibition of cell mobility and invasiveness *in vitro*.

EXPERIMENTAL SECTION

Instrumental Measurements. The C, H, and N analyses were performed with a Carlo Erba model EA 1108 microanalyzer. The ^{1}H, ^{13}C, ^{31}P, ^{19}F, and ^{195}Pt NMR spectra were recorded on a Bruker AC 300E or a Bruker AV 400 spectrometer. Chemical shifts are cited relative to $SiMe_4$ (^{1}H and ^{13}C, external), $CFCl_3$ (^{19}F, external), 85% H_3PO_4 (^{31}P, external), and $Na_2[PtCl_6]$ (^{195}Pt, external). ESI mass (positive mode) analyses were performed on a HPLC/MS TOF 6220. UV/vis spectroscopy was carried out on a PerkinElmer Lambda 750 S spectrometer with operating software. Fluorescence measurements were carried out with a PerkinElmer LS 55 50 Hz fluorescence spectrometer. An atomic absorption spectrometer (model 800, PerkinElmer, Shelton, USA) was used for the measurement of intracellular platinum concentrations.

Materials. Solvents were dried by the usual methods. The fluoroamines,[36] [Pt(dmba)(μ-Cl)]$_2$ (**1**),[37] and [Pt(dmba)(PPh_3)Cl] (**4**) were prepared by procedures described elsewhere. Sodium salt of calf thymus DNA, ethidium bromide (EB), and Hoechst 33258 were obtained from Sigma-Aldrich (Madrid, Spain); pBR322 plasmid DNA used in the studies was obtained from Boehringer-Mannheim (Mannheim, Germany).

Synthesis of the Dimeric Cycloplatinated(II) Complexes 2 and 3. The method of Ryabov was adapted.[37]

Complex 2. Yield: 35%. Anal. Calcd for **2** $C_{18}H_{22}N_2Cl_2F_2Pt_2$: C, 28.2; H, 2.90; N, 3.66. Found: C, 28.1; H, 2.86; N, 3.73. Positive-ion ESI mass spectra ion cluster (DMSO) at *m/z* 765.05 {[M]$^+$} $^+$.

Complex 3. Yield: 43%. Anal. Calcd for **3** $C_{20}H_{22}N_2Cl_2F_6Pt_2$: C, 27.76; H, 2.56; N, 3.24. Found: C, 27.63; H, 2.50; N, 3.28. ^{1}H NMR (600 MHz, $CDCl_3$, TMS): 7.0−7.3 (m, 6H, H^3, H^5 y H^6), 3.93 (s, 4H, CH_2N, J_{HPt} = 27.6 Hz), 2.95 (s, 12H $N(CH_3)_2$, J_{HPt} = 23.4 Hz). ^{13}C{^{1}H} NMR (150.90 MHz, $CDCl_3$, TMS): 121.0, 120.7, 120.6 (CH^3, CH^5 and CH^6), 75.1 (s, CH_2N) 53.9 (s, CH_3N). ^{19}F NMR (282.40 MHz, $CDCl_3$): −62.16 (s). Positive-ion ESI mass spectra ion cluster ($CHCl_3$) at *m/z* 865 {[M]$^+$} $^+$.

Synthesis of the Monomeric Cyclometalated Platinum(II) Complexes 5−11. A mixture of [Pt(C−N)(μ-Cl)]$_2$ (0.095 mmol) and the corresponding phosphine (0.200 mmol) in 8 mL of CH_2Cl_2 was stirred for 90 min at room temperature to yield a solution, which was partially evaporated under vacuum, and hexane was added to

dx.doi.org/10.1021/ic401973k | *Inorg. Chem.* 2013, 52, 13529−13535

precipitate the complexes as white solids, which were collected by filtration and air-dried.

Complex ***5***. Yield: 87%. Anal. Calcd for **5** $C_{27}H_{26}NClFPPt$: C, 50.3; H, 4.06; N, 2.17. Found: C, 50.1; H, 3.59; N, 2.21. ^{1}H NMR (300 MHz, $CDCl_3$, TMS): 7.69 (m, 6H, H_o PPh_3), 7.36 (m, 9H, H_p and H_m PPh_3), 6.98 (m, 1H, H^6), 6.52 (m, 1H, H^5), 6.06 (m, 1H, H^3, Pt satellites are observed as shoulders), 4.04 (d, 2H, CH_2N, J_{HP} = 2.4, J_{HPt} = 13.8), 2.94 (d, 6H, $N(CH_3)_2$, J_{HP} = 3.0, J_{HPt} = 16.8). $^{13}C\{^1H\}$ NMR (75.46 MHz, $CDCl_3$, TMS): 135.2 (d, CH_o PPh_3, J_{CP} = 10.9), 130.6 (s, CH_p PPh_3), 127.8 (d, CH_m PPh_3, J_{CP} = 11.1), 123.4 (d, CH^3, J_{CP} = 19.8), 122.3 (d, CH^6, J_{CF} = 8.30), 109.4 (d, CH^5, J_{CF} = 22.3), 73.6 (s, CH_2N) 50.6 (d, CH_3N, J_{CP} = 2.5). ^{195}Pt NMR (86.18 MHz, $CDCl_3$): −4023 (d, J_{PtP} = 4244). ^{19}F NMR (282.40 MHz, $CDCl_3$): −117.7 (s). $^{31}P\{^1H\}$ NMR (121.49 MHz, $CDCl_3$): 19.98 (s, J_{PPt} = 4244). Positive-ion ESI mass spectra ion cluster ($CHCl_3$) at *m*/*z* 609 $\{[M - Cl - H]^+\}^+$.

Complex ***6***. Yield: 88%. Anal. Calcd for **6** $C_{28}H_{26}F_3ClPNPt$: C, 48.4; H, 3.77; N, 2.02. Found: C, 48.3; H, 3.63; N, 2.04. ^{1}H NMR (300 MHz, $CDCl_3$, TMS): 7.67 (m, 6H, H_o PPh_3), 7.35 (m, 9H, H_p and H_m PPh_3), 7.05 (s, 2H, H^5 and H^6, system not up to expectations), 6.64 (br s, 1H, H^3, J_{HP} coupling constant cannot be determined, Pt satellites are observed as shoulders), 4.06 (d, 2H CH_2N, J_{HP} = 2.4, J_{HPt} = 12.6), 2.95 (d, 6H, $N(CH_3)_2$, J_{HP} = 2.7, J_{HPt} = 11.1). $^{13}C\{^1H\}$ NMR (75.46 MHz, $CDCl_3$, TMS): 135.0 (d, CH_o PPh_3, J_{CP} = 10.9), 133.3 (s, CH^3), 130.6 (s, CH_p PPh_3), 127.9 (d, CH_m PPh_3, J_{CP} = 11.2), 121.5 (s, CH^5 or CH^6), 114.1 (s, CH^5 or CH^6), 74.3 (s, CH_2N) 50.7 (s, CH_3N). ^{195}Pt NMR (86.18 MHz, $CDCl_3$): −4018 (d, J_{PtP} = 4272). ^{19}F NMR (282.40 MHz, $CDCl_3$): −63.1 (s). $^{31}P\{^1H\}$ NMR (121.49 MHz, $CDCl_3$): 19.8 (s, J_{PPt} = 4272). Positive-ion ESI mass spectra ion cluster ($CHCl_3$) at *m*/*z* 659 $\{[M - Cl - H]^+\}^+$.

Complex ***7***. Yield: 68%. Anal. Calcd for **7** $C_{30}H_{24}NClF_9PPt$: C, 43.4; H, 2.9; N, 1.8. Found: C, 43.4; H, 3.0; N, 1.7. ^{1}H NMR (400 MHz, $CDCl_3$, TMS): 7.85 (m, 6 H, H_o PR_3), 7.65 (d, 6 H, H_m PR_3, J_{HmHo} = 8.4), 7.08 (dd, 1H, H^6, J_{H6H5} = 4.8, J_{H6H4} = 0.4), 6.88 (ft, 1H, H^5), 6.38 (ft, 1H, H^4), 6.29 (m, 1H, H^3, Pt satellites are observed as shoulders), 4.12 (d, 2 H CH_2N, J_{HP} = 3.2, J_{HPt} = 6.3), 2.98 (d, 6H $N(CH_3)_2$, J_{HP} = 3.2, J_{HPt} = 5.6). $^{13}C\{^1H\}$ NMR (150.9 MHz, $CDCl_3$, TMS): 137.0 (d, CH^3, J_{CP} = 6.2), 135.4 (d, CH_o PR_3, J_{CP} = 11.4), 125.6 (s, CH^4), 125.0 (d, CH_m PR_3, J_{CP} = 11.4, J_{CF} = 3.3), 123.8 (s, CH^5), 122.2 (s, CH^6), 74.6 (s, CH_2N) 51.0 (s, CH_3N). ^{195}Pt NMR (86.18 MHz, $CDCl_3$): −4066 (d, J_{PtP} = 4304). ^{19}F NMR (282.40 MHz, $CDCl_3$): −63.13 (s). $^{31}P\{^1H\}$ NMR (121.49 MHz, $CDCl_3$): 21.6 (s, J_{PPt} = 4304). Positive-ion ESI mass spectra ion cluster ($CHCl_3$) at *m*/*z* 795 $\{[M - Cl - H]^+\}^+$.

Complex ***8***. Yield: 90%. Anal. Calcd for **8** $C_{30}H_{23}NClF_{10}PPt$: C, 42.4; H, 2.73; N, 1.65. Found: C, 42.5; H, 2.53; N, 1.71. ^{1}H NMR (300 MHz, $CDCl_3$, TMS): 7.84 (m, 6H, H_o PR_3), 7.67 (m, 6H, H_m PR_3), 7.04 (m, 1H, H^6), 6.58 (m, 1H, H^5), 5.91 (m, 1H, H^3, Pt satellites are observed as shoulders), 4.09 (d, 2H, CH_2N dmba, J_{HP} =3.0, J_{HPt} = 13.5), 2.96 (d, 6H, $N(CH_3)_2$, J_{HP} = 3.0, J_{HPt} = 11.4). $^{13}C\{^1H\}$ NMR (75.46 MHz, $CDCl_3$, TMS): 135.3 (d, CH_o PR_3, J_{CP} = 11.6), 125.1 (d, CH_m PR_3, J_{CP} = 8.1), 123.0 (d, CH^3, J_{CP} = 21.4), 121.5 (s, CH^6), 110.1 (d, CH^5, J_{CF} = 22.3), 74.1 (s, CH_2N) 50.8 (s, CH_3N). ^{195}Pt NMR (86.18 MHz, $CDCl_3$): −4038 (d, J_{PtP} = 4626). ^{19}F NMR (282.40 MHz, $CDCl_3$): −63.4 (s, CF_3), −116.9 (s, F). $^{31}P\{^1H\}$ NMR (121.49 MHz, $CDCl_3$): 21.1 (s, J_{PPt} = 4626). Positive-ion ESI mass spectra ion cluster ($CHCl_3$) at *m*/*z* 813 $\{[M - Cl - H]^+\}^+$.

Complex ***9***. Yield: 77%. Anal. Calcd for **9** $C_{31}H_{23}ClNF_{12}PPt$: C, 41.4; H, 2.58; N, 1.56. Found: C, 41.2; H, 2.34; N, 1.61. ^{1}H NMR (300 MHz, $CDCl_3$, TMS): 7.81 (m, 6H, H_o PR_3), 7.65 (d, 6H, H_m, J_{HmHo}= 8.4 Hz), 7.11 (s, 2H, H^5 y H^6, system not up to expectations), 6.42 (br s, 1H, H^3, J_{HP} coupling constant cannot be determined, Pt satellites are observed as shoulders), 4.11 (d, 2H CH_2N, J_{HP} = 2.7, J_{HPt} = 14.1), 2.96 (d, 6H $N(CH_3)_2$, J_{HP} = 3.0, J_{HPt} = 11.7). $^{13}C\{^1H\}$ NMR (75.46 MHz, $CDCl_3$, TMS): 135.2 (d, CH_o, J_{CP} = 11.5), 133.1 (s, CH^3), 125.1 (d, CH_m PPh_3, J_{CP} = 14.9), 122.0 (s, CH^5 or CH^6), 120.4 (s, CH^5 or CH^6), 77.1 (s, CH_2N), 50.9 (d, CH_3N, J_{CP} = 2.6). ^{195}Pt NMR (86.18 MHz, $CDCl_3$): −4027 (d, J_{PtP} = 4562). ^{19}F NMR (282.40 MHz, $CDCl_3$): −63.7 (s). $^{31}P\{^1H\}$ NMR (121.49 MHz, $CDCl_3$): 20.4 (s, J_{PPt} = 4562). Positive-ion ESI mass spectra ion cluster ($CHCl_3$) at *m*/*z* 863 $\{[M - Cl - H]^+\}^+$.

Complex ***10***. Yield: 60%. Anal. Calcd for **10** $C_{27}H_{24}NClF_3PPt$: C, 47.6; H, 3.6; N, 2.1. Found: C, 47.8; H, 3.4; N, 2.1. ^{1}H NMR (400 MHz, $CDCl_3$, TMS): 7.69 (m, 6H, H_o PPh_3), 7.06 (m, 7H, H_m PR_3 and H^6), 6.86 (m, 1H, H^5), 6.37 (m, 2H, H^4 y H^3 Pt satellites are observed as shoulders), 4.08 (d, 2H CH_2N, J_{HP} = 3, J_{HPt} = 30), 2.97 (d, 6H $N(CH_3)_2$, J_{HP} = 2.7, J_{HPt} = 23.7). $^{13}C\{^1H\}$ NMR (150.9 MHz, $CDCl_3$, TMS): 137.2 (m, CH^4 or CH^3 + CH_o PR_3), 125.3 (d, CH^4 or CH^3, J_{CP} = 10), 123.3 (s, CH^5), 121.9 (s, CH^6), 115.3 (m, CH_m), 74.3 (d, CH_2N, J_{CP} = 13.6), 50.9 (d, CH_3N, J_{CP} = 11.2). ^{195}Pt NMR (86.18 MHz, $CDCl_3$): −4055 (d, J_{PtP} = 4299). ^{19}F NMR (282.40 MHz, $CDCl_3$): −108.5 (s). $^{31}P\{^1H\}$ NMR (121.49 MHz, $CDCl_3$): 18.5 (s, J_{PPt} = 4299). Positive-ion ESI mass spectra ion cluster ($CHCl_3$) at *m*/*z* 645 $\{[M - Cl - H]^+\}^+$.

Complex ***11***. Yield: 68%. Anal. Calcd for **11** $C_{33}H_{21}NClF_{18}PPt$: C, 38.3; H, 2.1; N, 1.4. Found: C, 38.3; H, 1.9; N, 1.4. ^{1}H NMR (300 MHz, $CDCl_3$, TMS): 8.13 (d, 6H, H_o PR_3, J_{HP} = 11.1), 8.04 (s, 3H, H_p PR_3), 7.13 (d, 1H, H^6, J_{H6H5} = 7.5), 6.93 (ft, 1H, H^5), 6.37 (ft, 1H, H^4), 6.04 (dd, 1H, H^3, J_{H3H4} = 7.8, J_{H3H5} = 3.3, J_{HPt} = 53.7 Hz), 4.19 (d, 2H CH_2N, J_{HP} =3, J_{HPt} = 33.9), 2.99 (d, 6H $N(CH_3)_2$, J_{HP} = 2.7, J_{HPt} = 28.2). $^{13}C\{^1H\}$ NMR (150.9 MHz, $CDCl_3$, TMS): 136.4 (d, CH^3, J_{CP} = 22.0), 134.6 (d, CH_o PR_3, J_{CP} = 58.4), 125.9 (s, CH^4 + CH_p PR_3), 124.5 (s, CH^5), 122.8 (s, CH^6), 74.5 (d, CH_2N, J_{CP} = 14) 51.0 (d, CH_3N, J_{CP} = 10.4). ^{195}Pt NMR (86.18 MHz, $CDCl_3$): −4093 (d, J_{PtP} = 4352). ^{19}F NMR (282.40 MHz, $CDCl_3$): −63.2 (s). $^{31}P\{^1H\}$ NMR (121.49 MHz, $CDCl_3$): 25.6 (s, J_{PPt} = 4352). Positive-ion ESI mass spectra ion cluster ($CHCl_3$) at *m*/*z* 999 $\{[M - Cl - H]^+\}^+$.

Reactions of the Platinum(II) Complexes with 9-Ethylguanine Followed by ^{1}H NMR and ESI-MS. The reaction was carried out in an NMR tube containing D_2O and DMSO-d_6 (5%) as solvents. 9-Ethylguanine was incubated with the complexes in a ratio 2:1 in the above solvent mixture at 37 °C. The concentration of complexes for NMR was 1.0 mM. The reaction was followed for 24 h. The concentration of complexes for ESI-MS studies was 0.1 mM, and the ratio of 9-ethylguanine was 5:1.

X-ray Crystal Structure Analysis. Suitable crystals of **7**·2CH_2Cl_2 were grown from dichloromethane/hexane. A colorless needle crystal of 0.25 × 0.07 × 0.04 mm^3, immersed in Flombyl, was mounted on glass fibers and transferred to the cold gas stream of the diffractometer, Bruker Smart APEX. Data were recorded with Mo Kα radiation (λ = 0.71073 Å) in ω scan mode. Absorption correction for the compound was based on multiscans. The structure was solved by direct methods (SHELXS-97);[38] refinement was done by full-matrix least-squares on F^2 using the SHELXL-97 program suite with empirical (multiscan) absorption correction with SADABS (Bruker).[39] All non-hydrogen positions were refined with anisotropic temperature factors. Hydrogen atoms for aromatic CH, aliphatic CH_2, and CH_3 groups were positioned geometrically (C−H = 0.95 Å for aromatic CH, C−H = 0.99 Å for CH_2, C−H = 0.98 Å for CH_3) and refined using a riding model (AFIX 43 for aromatic CH, AFIX 23 for CH_2, AFIX 137 for CH_3), with $U_{iso}(H)$ = 1.2U_{eq}(CH, CH_2) and $U_{iso}(H)$ = 1.5U_{eq}(CH_3). Details of the X-ray structure determinations and refinements are provided in Table 3. Graphics were drawn with DIAMOND (Version 3.2).[40]

The temperature factors of one CF_3 group indicate a rotational disorder, which was, however, not refined further. The largest residual electron density peaks Q1 and Q2 are in the vicinities of these atoms and are further evidence of this disorder.

Supplementary crystallographic data for this paper have been deposited at Cambridge Crystallographic Data Centre (CCDC 948963) and can be accessed at www.ccdc.cam.ac.uk/data_request/cif.

Cell Line and Culture. The T47D human mammary adenocarcinoma cell line used in this study was grown in RPMI 1640 medium supplemented with 10% (v/v) fetal bovine serum (FBS) and 0.2 unit/mL bovine insulin in an atmosphere of 5% CO_2 at 37 °C. The human ovarian carcinoma cell lines (A2780 and A2780cisR) used in this study were grown in RPMI 1640 medium supplemented with 10% (v/v) fetal bovine serum (FBS) and 2 mM L-glutamine in an atmosphere of 5% CO_2 at 37 °C.

Table 3. Crystal Structure Determination Details for 7·2CH_2Cl_2

empirical formula	$C_{32}H_{28}Cl_5F_9NPPt$
fw [g/mol]	1000.86
cryst system	monoclinic
a [Å]	13.6261(12)
b [Å]	20.2034(17)
c [Å]	14.4902(12)
β [deg]	115.163(1)
V [Å^3]	3610.5(5)
temp (K)	100(2)
space group	$P2(1)/n$
Z	4
μ [mm^{-1}]	4.373
reflns collected	36873
indep reflns	6979
R(int)	0.0358
params	444
R1 [$I > 2\sigma(I)$][a]	0.0562
R1 (all data)	0.0597
wR2 [$I > 2\sigma(I)$]	0.1450
wR2 (all data)	0.1470
GOF[b]	1.145

[a] $R1 = \sum||F_o| - |F_c||/\sum|F_o|$; $wR2 = [\sum[w(F_o^2 - F_c^2)^2]/\sum w(F_o^2)^2]^{0.5}$. [b] Goodness-of-fit $= [\sum[w(F_o^2 - F_c^2)^2]/(n-p)]^{1/2}$.

Cytotoxicity Assay. Cell proliferation was evaluated by assay of crystal violet. T47D cells plated in 96-well sterile plates at a density of 5×10^3 cells/well with 100 μL of medium and were then incubated for 48 h. After attachment to the culture surface, the cells were incubated with various concentrations of the compounds tested freshly dissolved in DMSO and diluted in the culture medium (DMSO final concentration 1%) for 48 h at 37 °C. The cells were fixed by adding 10 μL of 11% glutaraldehyde. The plates were stirred for 15 min at room temperature and then washed 3−4 times with distilled water. The cells were stained with 100 μL of 1% crystal violet. The plates were stirred for 15 min and then washed 3−4 times with distilled water and dried. Then 100 μL of 10% acetic acid was added, and it was stirred for 15 min at room temperature.

Absorbance was measured at 595 nm in a Tecan Ultra Evolution spectrophotometer.

The effects of complexes were expressed as corrected pertentage inhibition values according to the following equation,

$$(\%)\ \text{inhibition} = [1 - (T/C)] \times 100$$

where T is the mean absorbance of the treated cells and C the mean absorbance in the controls.

The inhibitory potential of compounds was measured by calculating concentration−percentage inhibition curves; these curves were adjusted to the following equation:

$$E = E_{max}/[1 + (IC_{50})/C^n]$$

where E is the percentage inhibition observed, E_{max} is the maximal effect, IC_{50} is the concentration that inhibits 50% of maximal growth, C is the concentration of compounds tested, and n is the slope of the semilogarithmic dose−response sigmoid curves. This nonlinear fitting was performed using GraphPad Prism 2.01, 1996 software (GraphPad Software Inc.).

For comparison purposes, the cytotoxicity of cisplatin was evaluated under the same experimental conditions. All compounds were tested in two independent studies with triplicate points. The *in vitro* studies were performed in the USEF platform of the University of Santiago de Compostela (Spain).

Cell Cycle Arrest. Cell cycle arrest studies were performed on A2780 colon cancer cells. Typically, 3×10^5 cells were seeded in a 6-well plate with RPMI 1640 medium (5 mL/plate). Cells were allowed to fix to the plate by incubation for 24 h at 37 °C (5% CO_2). Then, the compounds **7**, **8**, and **9** were added at final concentrations coincident with their respective IC_{50} values in the different plates. Two plates were untreated, for being used as a blank (without any posterior treatment of any dye) and as a control. The cultures were incubated for an additional 48 h in the same conditions as described above. At this point, the medium was removed and stored in 15 mL falcons. Immediately, the fixed cells were treated with 1 mL of trypsin for 4 min at 37 °C and then 1 mL of RPMI 1640 medium containing FBS was added to stop the enzymatic action. The resulting 2 mL was added to the 15 mL falcon. In this way, both possible floating cells and adherent cells were considered for the assay. Cells were centrifuged (200g, 10 min), and the precipitated cells were washed with 2 mL of PBS. After another centrifugation (same conditions) and removing the supernatant, cells were resuspended in 200 μL of PBS. Then, 2 mL of a PBS/ethanol mix solution (70/30) was added to the cells. The solution was kept in ice for 30 min. The supernatant was eliminated by centrifugation (same conditions). The cells were again resuspended with 800 μL of PBS: Finally, 100 μL of an RNase solution (1 mg/mL) and 100 μL of a propidium iodide solution (400 μg/mL) were added. After stirring, the resulting suspension was incubated at 37 °C for 30 min at dark. Stained cells were then analyzed in a Becton-Dickinson FACScalibur flow cytometer.

Apoptosis Assays. For apoptosis determination assays, 10^5 cells were typically seeded in a 6-well plate. A2780 cells without (blank and control) and with compounds were incubated, collected, and washed once with PBS as described above (no PBS/ethanol mix was used in this case). After removing the PBS, 100 μL of a solution containing annexin V and IP (Annexin-V-Fluos from Roche) was added to the cell pellet. Cells were resuspended in this solution and left at room temperature in the dark for 15 min. PBS (200 μL) was added immediately prior to the measurements. These were carried out in a Beckman Coulter Epics XL flow cytometer, registering the emission at wavelengths of 620 and 525 nm for IP and annexin V, respectively. In each case, 10000 events were acquired.

Platinum Cellular Accumulation Studies. One million A2780 cells were incubated with 100 μM platinum complex at 10, 30, 60, 120, and 240 min. At each time point, the medium was discarded, and the cells were washed with 1 mL of ice-cold phosphate-buffered saline (PBS; pH 7.4). Then, cells were trypsinized, resuspended in 1 mL of RPMI 1640 medium, and centrifuged for 1 min at 4 °C and 1500g. The supernatant was discarded, and the pellet was washed twice in 1 mL of ice-cold PBS. At this point, cells were counted. After centrifugation for 1 min at 18000g, the supernatant was discarded again, and the cell pellet was frozen at −80 °C until further analysis. Immediately after thawing, the cells were lysed with concentrated nitric acid for 1 h in a water bath at 80 °C. Afterward, intracellular platinum concentrations were measured by flameless atomic absorption spectrometry. An atomic absorption spectrometer (model 800, PerkinElmer, Shelton, USA) equipped for Zeeman-effect background correction with a transversely heated graphite tube atomizer and AS-800 autosampler was used. The autosampler was not used, and the samples were pipetted manually into the atomizer. Pyrolytic graphite platforms in pyrolytically coated tubes were obtained from the same manufacturer (part number B050-4033). Argon at 250 mL min^{-1} was used as inert gas, except during atomization, when it was stopped. Platinum hollow cathode lamps (PerkinElmer) were used as the radiation sources.

Electrophoretic Mobility Study. pBR322 plasmid DNA of 0.25 μg/μL concentration was used for the experiments. Four microliters of charge maker (Lambda−pUC Mix marker) was added to aliquots of 20 μL of the drug−DNA complex. The iridium complexes were incubated at the molar ratio $r_i = 0.50$ with pBR322 plasmid DNA at 37 °C for 24 h. The mixtures underwent electrophoresis in agarose gel 1% in 1× TBE buffer (45 mM Tris-borate, 1 mM EDTA, pH 8.0) for 5 h at 30 V. Gel was subsequently stained in the same buffer containing ethidium bromide (1 μg/mL) for 20 min. The DNA bands were visualized with an AlphaImager EC (Alpha Innotech).

Cathepsin B Inhibition Assay. Crude bovine spleen cat B was purchased from Sigma (C6286) and used without further purification.

dx.doi.org/10.1021/ic401973k | *Inorg. Chem.* 2013, 52, 13529−13535

The colorimetric cat B assay was performed in 100 mM sodium phosphate, 1 mM EDTA, 0.025% polyoxyethylene (23) lauryl ether (BRIJ), pH = 6, using Z-L-Lys-ONp hydrochloride (Sigma C3637) as substrate. For the enzyme to be catalytically functional, the active site cysteine needs to be in a reduced form. Therefore, before using, cat B was prereduced with dithiothreitol (DTT) to ensure that the majority of the enzyme is in a catalytically active form. Thus, cat B was activated, before dilution, in the presence of excess DTT for 1 h at 30 °C.

IC_{50} determinations were performed in duplicate using a fixed enzyme concentration of 1 μM, and a fixed substrate concentration of 0.08 mM. Inhibitor concentrations ranged from 1 to 50 μM. The enzyme and inhibitor were co-incubated at 25 °C over a period of 24 h prior to the addition of substrate. Activity was measured over 1 min at 326 nm.

Cysteine reactivation was evaluated using an inhibitor concentration corresponding to 2 × IC_{50}. The enzyme was preincubated with an excess of DTT (Sigma D0632) for 1 h at 30 °C. After the activation, the enzyme and the compound were incubated at 25 °C for 24 h. Then, 1 mM L-cysteine was added and incubated at different times, 1, 2, 3, 4, 6, and 24 h, at 25 °C. Following incubation, the substrate was added, and activity was assessed.

■ ASSOCIATED CONTENT

Ⓢ Supporting Information

Structures, energies, and Cartesian coordinates for all computed compounds. This material is available free of charge via the Internet at http://pubs.acs.org.

■ AUTHOR INFORMATION

Corresponding Author

*E-mail: jruiz@um.es. Fax: +34 868 884148. Tel: +34 868 887455.

Notes

The authors declare no competing financial interest.

■ ACKNOWLEDGMENTS

This work was supported by the Spanish *Ministerio de Economía y Competitividad* and FEDER (Project SAF2011-26611) and by Fundación Séneca-CARM (Projects 08666/PI/08 and 15354/PI/10) and also has been partially funded by the European Union Seventh Framework Programme-Marie Curie CO-FUND (FP7/2007-2013) under UMU Incoming Mobility Programme ACTion (U-IMPACT) Grant Agreement 267143 and COST ACTION CM1105 for providing opportunities of discussion.

■ REFERENCES

(1) Muggia, F. *Gynecol. Oncol.* **2009**, *112*, 275−281.
(2) Fuertes, M. A.; Castilla, J.; Alonso, C.; Pérez, J. M. *Curr. Med. Chem.* **2003**, *10*, 257−266.
(3) Berners-Price, S. J. *Angew. Chem., Int. Ed.* **2011**, *50*, 804−805.
(4) Todd, R. C.; Lippard, S. J. *Metallomics* **2009**, *1*, 280−291.
(5) Arnesano, F.; Natile, G. *Pure Appl. Chem.* **2008**, *80*, 2715−2725.
(6) Jakupec, M. A.; Galanski, M.; Arion, V. B.; Hartinger, C. G.; Keppler, B. K. *Dalton Trans.* **2008**, 183−194.
(7) Sánchez-Cano, C.; Hannon, M. J. *Dalton Trans.* **2009**, 10702−10711.
(8) Ott, I.; Gust, R. *Arch. Pharm.* **2007**, *340*, 117−126.
(9) Bruijnincx, P. C. A.; Sadler, P. J. *Curr. Opin. Chem. Biol.* **2008**, *12*, 197−206.
(10) Gasser, G.; Ott, I.; Metzler-Nolte, N. *J. Med. Chem.* **2011**, *54*, 3−25.
(11) Hartinger, C. G.; Metzler-Nolte, N.; Dyson, P. J. *Organometallics* **2012**, *31*, 5677−5685.
(12) Meggers, E. *Curr. Opin.Chem.* **2007**, *11*, 287−292.
(13) Hannon, M. J. *Pure Appl. Chem.* **2007**, *79*, 2243−2261.
(14) Cutillas, N.; Yellol, G. S.; de Haro, C.; Vicente, C.; Rodríguez, V.; Ruiz, J. *Coord. Chem. Rev.* **2013**, *257*, 2784−2797.
(15) Wilson, J. J.; Lippard, S. J. *J. Med. Chem.* **2012**, *55*, 5326−5336.
(16) Crespo, M. *Organometallics* **2012**, *31*, 1216−1234.
(17) Salwiczek, M.; Nyakatura, E. K.; Gerling, U. I. M.; Ye, S.; Koksch, B. *Chem. Soc. Rev.* **2012**, *41*, 2135−2171.
(18) Ruiz, J.; Rodríguez, V.; de Haro, C.; Espinosa, A.; Pérez, J.; Janiak, C. *Dalton Trans.* **2010**, *39*, 3290−3301.
(19) Ruiz, J.; Lorenzo, J.; Vicente, C.; López, G.; López-De-Luzuriaga, J. M.; Monge, M.; Avilés, F. X.; Bautista, D.; Moreno, V.; Laguna, A. *Inorg. Chem.* **2008**, *47*, 6990−7001.
(20) Ruiz, J.; Rodríguez, V.; Cutillas, N.; López, G.; Bautista, D. *Inorg. Chem.* **2008**, *47*, 10025−10036.
(21) Meijer, M. D.; Kleij, A. W.; Williams, B. S.; Ellis, D.; Lutz, M.; Spek, A. L.; van Klink, G. P. M.; van Koten, G. *Organometallics* **2002**, *21*, 264−271.
(22) Ruiz, J.; Villa, M. D.; Rodríguez, V.; Cutillas, N.; Vicente, C.; López, G.; Bautista, D. *Inorg. Chem.* **2007**, *46*, 5448−5449.
(23) Althoff, G.; Ruiz, J.; Rodríguez, V.; López, G.; Pérez, J.; Janiak, C. *CrystEngComm* **2006**, *8*, 662−665.
(24) Bedford, R. B.; Betham, M.; Butts, C. P.; Coles, S. J.; Hursthouse, M. B.; Scully, P. N.; Tucker, J. H. R.; Wilkie, J.; Willener, Y. *Chem. Comm* **2008**, 2429−2431.
(25) Nishio, M. *CrystEngComm* **2004**, *6*, 130−158.
(26) Hathwar, V. R.; Guru Row, T. N. *Cryst. Growth Des.* **2011**, *11*, 1528−7483.
(27) Loh, S. Y.; Mistry, P.; Kelland, L. R.; Abel, G.; Harrap, K. R. *Br. J. Cancer.* **1992**, *66*, 1109−1115.
(28) Goddard, P. M.; Orr, R. M.; Valenti, M. R.; Barnard, C. F.; Murrer, B. A.; Kelland, L. R.; Harrap, K. R. *Anticancer Res.* **1996**, *16*, 33−38.
(29) Behrens, B. C.; Hamilton, T. C.; Masuda, H.; Grotzinger, K. R.; Whang-Peng, J.; Louie, K. G.; Knutsen, T.; McKoy, W. M.; Young, R. C.; Ozols, R. F. *Cancer Res.* **1987**, *47*, 414−418.
(30) Kelland, L. R.; Barnard, C. F. J.; Mellish, K. J.; Jones, M.; Goddard, P. M.; Valenti, M.; Bryant, A.; Murrer, B. A.; Harrap, K. R. *Cancer Res.* **1994**, *54*, 5618−5622.
(31) Romero-Canelón, I.; Salassa, L.; Sadler, P. J. *J. Med. Chem.* **2013**, *56*, 1291−1300.
(32) Ushay, H. M.; Tullius, T. D.; Lippard, S. J. *Biochemistry* **1981**, *20*, 3744−3748.
(33) Fernández, P.; Farre, X.; Nadal, A.; Fernández, E.; Peiro, N.; Sloane, B. F.; Sih, G.; Chapman, H. A.; Campo, E.; Cardesa, A. *Int. J. Cancer* **2001**, *95*, 51−55.
(34) Podgorski, I.; Sloane, B. F. *Biochem. Soc. Symp.* **2003**, *70*, 263−276.
(35) Casini, A.; Gabbiani, C.; Sorrentino, F.; Rigobello, M. P.; Geldbach, A. B. T. J.; Marrone, A.; Re, N.; Hartinger, C. G.; Dyson, P. J.; Messori, L. *J. Med. Chem.* **2008**, *51*, 6773−6781.
(36) De Vries, T. S.; Prokofjevs, A.; Harvey, J. N.; Vedejs, E. *J. Am. Chem. Soc.* **2009**, *131*, 14679−14687.
(37) Ryabov, A. D.; Kuz'mina, L. G.; Dvortsova, N. V.; Stufkens, D. J.; van Eldik, R. *Inorg. Chem.* **1993**, *32*, 3166−3174.
(38) Sheldrick, G. M. *Acta Crystallogr.* **2008**, *A64*, 112.
(39) Sheldrick, G. M. Program SADABS, University of Göttingen, Göttingen, Germany, 1996.
(40) DIAMOND 3.2 for Windows. Crystal Impact Gbr, Bonn, Germany; http://www.crystalimpact.com/diamond.